We are IntechOpen, the world's leading publisher of Open Access books Built by scientists, for scientists

4,800
Open access books available

122,000
International authors and editors

135M
Downloads

Our authors are among the

154
Countries delivered to

TOP 1%
most cited scientists

12.2%
Contributors from top 500 universities

CLARIVATE ANALYTICS BOOK CITATION INDEX INDEXED

WEB OF SCIENCE™

Selection of our books indexed in the Book Citation Index in Web of Science™ Core Collection (BKCI)

Interested in publishing with us?
Contact book.department@intechopen.com

Numbers displayed above are based on latest data collected.
For more information visit www.intechopen.com

Chapter 8

Quantitative Proteomic Analysis of Skeletal Muscle Detergent-Resistant Membranes in a Smith-Lemli-Opitz Syndrome Mouse

Maria Luís Cardoso, Rui Vitorino, Henrique Reguengo, Susana Casal, Rui Fernandes, Isabel Duarte, Sofia Lamas, Renato Alves, Francisco Amado and Franklim Marques

Additional information is available at the end of the chapter

http://dx.doi.org/10.5772/intechopen.78037

Abstract

Smith-Lemli-Opitz syndrome (SLOS) is an inborn error of metabolism affecting the last step of cholesterol biosynthesis. It is characterized by a deficiency of the enzyme 7-dehydrocholesterol reductase and accumulation of 7-dehydrocholesterol (7DHC) in cells and body fluids. Given the similarities between 7DHC and cholesterol, 7DHC can be incorporated into cell membranes in lieu of cholesterol. Nevertheless, due to their structural differences and distinct affinity to other membrane components, this substitution alters membrane properties and one can expect to find abnormalities in membrane protein composition. In order to identify differences in membrane proteins that could facilitate our understanding of SLOS physiopathology, we isolated detergent-resistant membranes (DRMs) from the skeletal muscle of *Dhcr7*$^{T93M/T93M}$ mice and C57/BL6 controls and performed comparative proteomic analysis using iTRAQ for peptide quantification. A total of 133 proteins were identified in the DRM fraction: 17 (13%) proteins demonstrated increased expression in SLOS mice, whereas, 21 (16%) showed decreased expression. Characterization of functional point of view and bioenergetics pathway and transmembrane transport responded to the major differences between the two groups of animals.

Keywords: skeletal muscle, detergent-resistant membranes (DRMs), Smith-Lemli-Opitz syndrome, SLO, comparative proteomics, mouse model, *Dhcr7*$^{T93M/T93M}$

1. Introduction

Smith-Lemli-Opitz syndrome (SLOS), OMIM #270400, is one of the nine known disorders associated with altered post-squalene cholesterol biosynthesis [1, 2]. This autosomal recessive genetic disease was first described in 1964, as a syndrome of cognitive impairment and multiple malformations [3]. Thirty years were needed to further characterize the disorder as a metabolic disease and identify the underlying enzymatic defect. SLOS is caused by deficiency of 7-dehydrocholesterol redutase (7-DHCR, 3-hydroxysteroid redutase, EC.1.3.1.21) which catalyzes the conversion of 7-dehydrocholesterol (7DHC) to cholesterol, the terminal step of Kandutsch-Russell pathway [4, 5]. Consequently, SLOS patients typically show increased 7DHC and decreased serum and tissue cholesterol levels [5]. In 1998, mutations of the 3β-hydroxysterol Δ7-reductase gene (*DHCR7*) were shown to cause SLOS [6–8] and more than 154 *DHCR7* mutations have been so far identified in SLOS patients [9]. The development of animal models has improved the understanding of SLOS physiopathology and provided material for *in vivo* and *in vitro* investigation of biological consequences of cholesterol deficiency. In 2001, two mouse models with null mutations in *Dhcr7* gene have been created by homologous recombination [10, 11]. The malformations in the null mice are very mild compared to what would be seen in a null human infant (i.e., SLO type II). The mutant mice died within the first 24 h of extra-uterine life. Later, a mouse model with a milder phenotype was developed [12]. This hypomorphic mouse has a missense mutation equivalent to the human p.T93M, previously identified in SLOS patients often with Mediterranean heritage [13–15]. Like the majority of SLOS patients, the SLOS mouse models manifest a deficiency in cholesterol biosynthesis resulting in low levels of cholesterol in serum and tissues [11].

Effective cholesterol biosynthesis is especially critical at certain stages during development and continues to be important throughout life [16], since cholesterol is an essential lipid with multiple functions. Cholesterol is a major lipid component of membrane microdomains, which are crucial cell-surface dynamic structures responsible for many cellular signaling and communication events [17]. Membrane domains can form through a number of mechanisms involving lipid-lipid and protein-lipid interactions. One type of membrane domain is the cholesterol-dependent membrane raft [18]. Properties of these membrane domains have been primarily inferred from the study of detergent-resistant membranes (DRMs), composed by the non-ionic-detergent insoluble, low-buoyant density membranous fractions of cells [19]. Although it was initially thought that such microdomains enriched in cholesterol exist exclusively in the plasma membrane, increasing evidence suggests that similar lipid microdomains (sometimes referred as raft-like microdomains) are also present in internal organelles [20–22] with some of them being involved in the crosstalk between organelles [23].

Proteomics constitutes a powerful tool to study complex biological mechanisms and to identify alterations in protein expression induced by changes in the environment, drugs, or disease states. As such, proteomics is now widely employed to help understand pathological processes induced by the disease [24–27]. The effect of an inborn error of cholesterol synthesis on skeletal muscle has not previously been reported. In this chapter, we report a comparative analysis of protein expression in skeletal muscle DRMs isolated from *Dhcr7* T93M homozygous mutant

http://dx.doi.org/10.5772/intechopen.78037

mice (*Dhcr7*$^{T93M/T93M}$) and wild type controls (*Dhcr7*$^{+/+}$) controls. We analyzed sterols by GC–MS and we used amine-reactive isobaric tagging reagents (iTRAQ) for quantitative subcellular proteomics. We found the altered expression of key muscle proteins involved with bioenergetics, membrane transport and Ca^{2+} homeostasis.

2. Material and methods

2.1. Materials

Butylhydroxytoluene (BHT), N,O-bis(trimethylsilyl) trifluoroacetamide (BSTFA), triethylammonium bicarbonate (TEAB), trifluoroacetic acid (TFA), α-cyano-4-hydroxycinnamic acid (α-CHCA), 3-[(3-cholamidopropyl)dimethylammonio]-1-propanesulfonate (CHAPS), protease inhibitor cocktail, formic acid and urea were purchased from Sigma (Karlsruhe, Germany). RC DC Protein Assay kit for protein quantification was from BioRad lab (Hercules, USA). The iTRAQ kit was purchased from Applied Biosystems (Foster City, CA). Sequencing grade modified trypsin (bovine) was from ABSciex (ABSciex, USA). HPLC-grade acetonitrile (ACN, Riedel, Seelze, Germany) and Milli-Q grade water were also used. Rabbit raised polyclonal anti-caveolin 1 (ab2910) and anti-annexin A2 antibodies were purchased from Abcom, Cambridge, UK. Analytical reagent grade chemicals were used unless stated otherwise.

2.2. Animals

The T93M mutation [12] was backcrossed into C57/BL6 for three generations. Homozygous (T93M/T93M) mice are viable and fertile [16]. Control C57/BL6 mice were obtained from IBMC Animal Centre from Oporto University.

All the animals were housed in plastic cages with free access to water and food (cholesterol free —chow -Mucedola, Ref: 4RF21). The animals were handled and maintained in controlled conditions according to international standards. Animals were euthanized using deep isoflurane anesthesia when they were 10 days old. Gastrocnemius and soleus muscles were dissected, submerged in ice-cold buffer (TRIS, HCl, pH 7.4, 10 mM mercaptoethanol, 0.28 M sucrose) and immediately frozen at −80°C.

2.3. DRMs extraction

Detergent-resistant membranes (DRMs) were isolated using cold Triton X-100 treatment followed by sucrose gradient centrifugation. In order to minimize individual variation, samples were analyzed as pools of several animals. The procedure was adapted from Kim et al. [28]. Briefly, the samples were allowed to thaw slowly on ice, and tissue from three mice (approximately 300 mg) was minced with scissors, mixed with 700 μL of cold (4°C) lysis buffer (25 nM HEPES-HCl, pH 6,5, 150 mM NaCl, 1 mM EDTA, 1% Triton X-100 and protease inhibitor cocktail) and homogenized 30 times with a Poter homogenizer. The sample was maintained in

an ice bath during homogenization and then incubated for 30 min at 4°C. Aliquots of this homogenate were collected for protein quantification and sterol analysis.

The resulting extract was mixed with an equal volume of cold sucrose 80% (w/v) to give a final sucrose concentration of 40%, transferred to the bottom of a ultra-centrifuge tube (Ultra-clear 14 × 89 mm, Beckman Ref 344059) and overlaid carefully with 6.0 mL 30% and 3.0 mL 5% cold sucrose solutions, containing 25 nM HEPES-HCl, pH 6.5, 150 mM NaCl, 1 mM EDTA, 1% Triton X-100. Discontinuous sucrose gradients were centrifuged for 20 h, at 187,000 g on a Sorvall Ultra Pro 80 UC, swinging bucket SW41 at 4°C. The DRMs fraction, which collects at the interface of the 5 and 30% sucrose layers, was isolated, washed with 9 mL of modified HEPES buffer and centrifuged 30 min at 49,500 g at 4°C. After centrifugation, the supernatant was discarded and the pellet containing purified DRMs was suspended in phosphate buffered saline (PBS) and stored frozen at −80°C until further proteomic or sterol analysis.

2.4. Sterols analysis

For extraction of neutral sterols, 50 μL of sample was mixed with 50 μL of BHT 0.05% in methanol (antioxidant), 50 μL of epicoprostanol 0.10 mmol/L (internal standard) and saponified at 60°C for 1 h by 16 adding 1 mL of 4% (w/v) KOH in 90% ethanol. The samples were then diluted with 1 mL of deionized water and the lipids were extracted twice with 2 mL of hexane. The pooled hexane extracts were dried under a gentle nitrogen stream at room temperature and derivatized with 50 μL BSTFA in 50 μL pyridine at 60°C for 1 h [29]. The trimethylsilylether derivatives of sterols were separated by GC–MS with a Supelco 28471_U SLB-5MS column (30 m × 0.32 mm i.d., 0.25 μm film thickness). The injector temperature was set at 270°C, and the splitless injection mode was used. The initial column temperature was 180°C for 1 min and programmed to increase at a rate of 20°C/min to 250°C and then increased again at 5°C/min rate till 300°C. The carrier gas was helium at a linear constant flow rate of 40 cm/s. The interface was programmed to 280°C, the quadrupole to 150°C and the ionization source to 230°C. After a solvent delay of 2.5 min, the eluted sterols were identified by their retention times (comparing with commercial standards) and respective mass spectra and quantified by selected ion monitoring (**Table 1**). The method was linear and reproducible for the range of amounts assayed.

Sterol	Retention time		m/z	
Epicoprostanol	13.02	**370**	257	355
Cholesterol	13.72	**329**	353	368
7DHC	14.02	**325**	351	366
Desmosterol	14.10	**343**	327	
Sitosterol	14.80	**357**	396	486
Lathosterol	15.80	**255**	443	458

The m/z ions selected for sterol quantification are printed in bold.

Table 1. Sterol parameters.

2.5. Proteomic profile

2.5.1. Pellet solubilization and protein quantification

Each assay involved four sample pools: a wt-BL6 control and a *Dhcr7*$^{T93M/T93M}$ and their duplicates. For protein extraction, the DRMs pellets were treated with 10 volumes (w/v) of solubilization buffer (7 M urea, 2 M thiourea, 1% (w/v) CHAPS, 1% (w/v) Triton X-100, 1% (v/v) ampholytes (3–10) and 1 mM TCEP), sonicated briefly, then incubated for 10 min at room temperature under agitation. Clear cell lysates were obtained by centrifugation at 12,000×*g* for 30 min at 4°C and saved for analysis. Insoluble material was discarded.

The protein concentration was determined by RC DC Protein Assay kit, using BSA to generate the calibration curve.

2.5.2. Sample preparation for mass spectrometry analysis

Reduction, alkylation and digestion steps were performed according to the protocol provided by the manufacturer. Briefly, 100 mg of DRM protein was mixed with TEAB buffer (1 M, pH 8.5) and an enhancer of enzymatic digestion RapiGest (Waters) to give a final concentration of 0.5 M and 0.1%, respectively. Samples were then treated with: (1) a reducing agent—TCEP 5 mM—used to break disulfide bonds within and between proteins, for 1 h at 37°C and (2) a cysteine (sulfhydryl group) blocking reagent—S-methyl methanethiosulfonate (MMTS) 10 mM—for 10 min, at room temperature. Then, 2 mg of trypsin was added to each sample and the digestion was performed for 18 h at 37°C. The digested tryptic specimens were dried using a Speed-Vac. iTRAQ labeling was carried out according to the instructions provided by the manufacturer. *Dhcr7*$^{T93M/T93M}$ mice DRMs samples were marked with iTRAQ Tags 116 and wt-BL6 with114 and the duplicates with 115 and 113, respectively. The labeled samples were combined in pairs and dried in a Speed-Vac. The peptides were separated by reverse-phase liquid chromatography as previously published [30].

2.5.3. LC-MS/MS analysis

Peptide mass spectra were obtained in the mass range 700–4500 Da on a MALDI-TOF/TOF mass spectrometer (4800 Proteomics Analyzer, Applied Biosystems, Foster City, CA, USA) in the positive ion reflector mode. The obtained spectra were processed and analyzed by the ProteinPilot® software (v4.0 AB Sciex, USA), which uses an algorithm for protein/peptide identification based on the comparison of MS/MS data against the SwissProt protein database [31].

Protein clustering was performed according to biological and molecular functions derived from the PANTHER classification system.

2.6. Immunocytochemistry assay

Immunocytochemistry assays were performed in order to confirm the presence of (1) caveolin-1, a protein marker of a subtype of membrane microdomains which are rich in cholesterol, designated caveolae (anti-caveolin-1 antibody dilution 1:500) and (2) annexin 2 another protein associated with enriched cholesterol microdomains, that was found increased in the SLO

mouse model (antibody dilution 1:2000). A sequential incubation with a secondary biotinylated anti-rabbit antibody was performed and diaminobenzidine (which stains brown) was employed as chromogen. Skeletal muscle samples were then counterstained with hematoxylin.

3. Results and discussion

3.1. Sterols

Sterols were extracted from two pools of biological samples: muscle homogenates and muscle DRMs, and then analyzed by GC-MS. Results are presented as the average ratios between sterols amounts. We observed a markedly elevated cholesterol/7DHC ratio in muscle homogenates from wild-type animals, reflecting the large amount of cholesterol and minimal levels of its precursor (7DHC), in controls. This ratio was also much greater than one in *Dhcr7*$^{T93M/T93M}$ mice, indicating that affected mice have significant residual 7-DHCR enzymatic activity and are thus capable of producing significant amounts of cholesterol (**Figure 1A**).

Desmosterol is a cholesterol precursor by an alternative biosynthetic route, and there are no significant differences in desmosterol levels between controls and affected animals. This is also reflected in the 7DHC/desmosterol ratio. This parameter showed an enrichment of *Dhcr7*$^{T93M/T93M}$ animals' DRMs in 7DHC (**Figure 1B**). The ratio 7DHC/cholesterol also indicates that 7DHC is preferentially incorporated in membrane microdomains (**Figure 1C**). These findings corroborate the previous ones published by Rakheja and Boriack, based on liver analysis of SLOS patients, which showed that 7DHC accumulates in hepatic DRMs [32]. Furthermore, while wt-BL6 controls have essentially only cholesterol in DRMs, affected mice present a mixture of cholesterol and 7DHC (**Figure 2**).

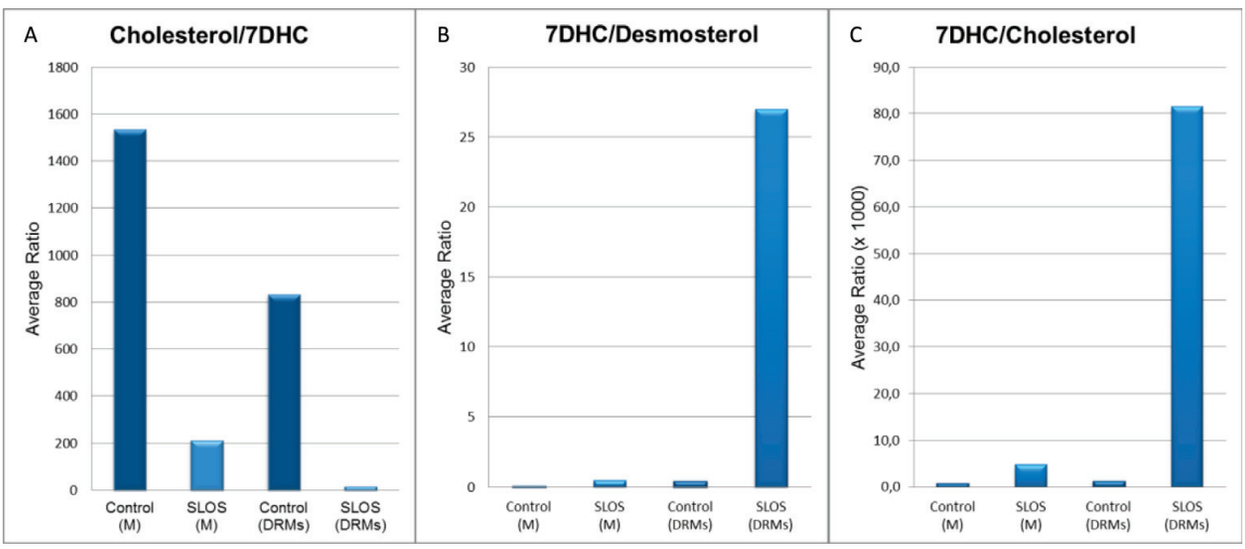

Figure 1. Average ratios between the amounts of: cholesterol and 7DHC (A), 7DHC and desmosterol (B) and 7DHC and cholesterol (C), extracted from skeletal muscle homogenates (M) and DRMs of wt-BL6 controls and hypomorphic *Dhcr7*$^{T93M/T93M}$ mice pooled samples.

3.2. Proteomics

In order to explore the protein changes on sarcolemma, due to decreased 7-DHCR activity, we analyzed DRMs utilizing iTRAQ labeling and LC-MS/MS.

A total of 133 unique proteins were identified. Those identified based on a single peptide and those with a protein score less than 2.5 fold were excluded. Then a cut-off of 30% was applied to iTRAQ average ratios allowing us to select proteins with an important variation in SLOS mice relatively to controls. Differential protein expression was specific and not just a general finding. Caveolin-1, a protein known to be expressed in cholesterol-rich membrane microdomains did not show differential expression (**Figure 3**).

Of the 133 identified proteins, we observed an altered expression of 38 (29%) proteins. Increased and decreased expression was observed for 17 and 21 proteins, respectively (**Table 2**). The replicate samples demonstrated a strong positive correlation (r = 0.90) and indicated good reproducibility (**Figure 4**).

Most proteins showing an altered expression in DRMs preparations were found to participate in at least one of three main cellular processes: membrane trafficking, energy production and Ca^{2+} homeostasis.

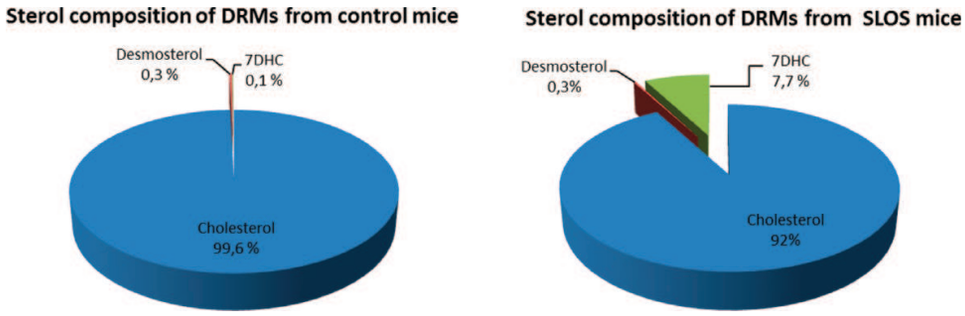

Figure 2. Comparative analysis of sterol composition of DRMs extracted from skeletal muscle of wt-BL6 controls and hypomorphic *DHCR7*$^{T93M/T93M}$ (SLOS) mice.

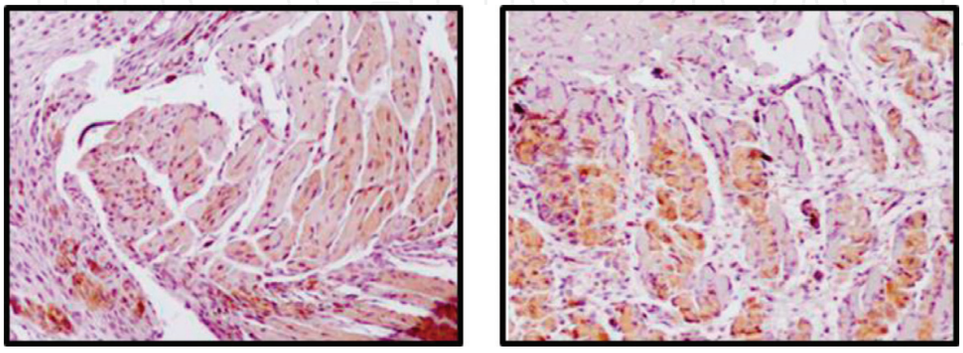

Figure 3. Immunohistochemical stain for caveolin-1 (×10) shows no significant differences between *Dhcr7* $^{93M/93M}$ (on the left) and wt-BL6 (on the right) skeletal muscle samples.

Total score	Sequence coverage %	Accession #		Name	Peptides (95%)	SLOS/wt-BL6
12.5	37	P07356	ANXA2_MOUSE	Annexin A2	15	6.2
6.6	29	P16858	G3P_MOUSE	Glyceraldehyde-3-phosphate dehydrogenase	4	5.2
51.2	50	Q8R429	AT2A1_MOUSE	Sarcoplasmic/endoplasmic reticulum calcium ATPase 1	85	3.9
11.6	53	P07310	KCRM_MOUSE	Creatine kinase M-type	12	2.7
6.7	41	P27573	MYP0_MOUSE	Myelin protein P0	10	2.0
18.5	37	Q8K2B3	DHSA_MOUSE	Succinate dehydrogenase [ubiquinone] flavoprotein subunit, mitochondrial	18	1.9
17.4	59	P51881	ADT2_MOUSE	ADP/ATP translocase 2	24	1.9
2.5	9	P09055	ITB1_MOUSE	Integrin beta-1	3	1.9
29.5	56	P56480	ATPB_MOUSE	ATP synthase subunit beta, mitochondrial	35	1.8
4.1	46	Q9D3D9	ATPD_MOUSE	ATP synthase subunit delta, mitochondrial	4	1.6
14,5	14	O09165	CASQ1_MOUSE	Calsequestrin-1	22	1.6
4,6	31	Q8C7E7	STBD1_MOUSE	Starch-binding domain-containing protein 1	7	1.5
10.0	17	P70302	STIM1_MOUSE	Stromal interaction molecule 1	7	1.5
25.4	70	P48962	ADT1_MOUSE	ADP/ATP translocase 1	39	1.5
6.4	33	Q8VEM8	MPCP_MOUSE	Phosphate carrier protein, mitochondrial	9	1.4
19.1	59	Q03265	ATPA_MOUSE	ATP synthase subunit alpha, mitochondrial	27	1.3
3.0	47	Q9CQQ7	AT5F1_MOUSE	ATP synthase subunit b1, mitochondrial	14	1.3
4.0	19	Q5U458	DJC11_MOUSE	DnaJ homolog subfamily C member 11	3	0.8
23.3	45	Q8BMK4	CKAP4_MOUSE	Cytoskeleton-associated protein 4	26	0.8
5.5	50	Q9CR68	UCRI_MOUSE	Cytochrome b-c1 complex subunit Rieske, mitochondrial	9	0.7
4.2	82	P99028	QCR6_MOUSE	Cytochrome b-c1 complex subunit 6, mitochondrial	13	0.7
5.0	73	P56391	CX6B1_MOUSE	Cytochrome c oxidase subunit 6B1	9	0.6
5.1	2	Q8VDD5	MYH9_MOUSE	Myosin-9	5	0.6
4.4	53	Q9DCS9	NDUBA_MOUSE	NADH dehydrogenase [ubiquinone] 1 beta subcomplex subunit 10	14	0.6
4.2	7	P99024	TBB5_MOUSE	Tubulin beta-5 chain	7	0.6
20.1	46	P08121	CO3A1_MOUSE	Collagen alpha-1(III) chain	25	0.6
26.0	56	Q9CZ13	QCR1_MOUSE	Cytochrome b-c1 complex subunit 1, mitochondrial	38	0.6
6.5	60	P97450	ATP5J_MOUSE	ATP synthase-coupling factor 6, mitochondrial	19	0.6
36.1	62	Q01149	CO1A2_MOUSE	Collagen alpha-2(I) chain	47	0.6
5.3	15	Q9Z239	PLM_MOUSE	Phospholemman	5	0.5

Total score	Sequence coverage %	Accession #		Name	Peptides (95%)	SLOS/wt-BL6
4.5	59	Q9CPQ1	COX6C_MOUSE	Cytochrome c oxidase subunit 6C	6	0.5
66.9	35	P13542	MYH8_MOUSE	Myosin-8	71	0.5
10.1	57	Q9D6J5	NDUB8_MOUSE	NADH dehydrogenase [ubiquinone] 1 beta subcomplex subunit 8, mitochondrial	13	0.5
3.0	29	Q99LY9	NDUS5_MOUSE	NADH dehydrogenase [ubiquinone] iron-sulfur protein 5	2	0.5
5.9	13	P68134	ACTS_MOUSE	Actin, alpha skeletal muscle	5	0.4
8.8	46	P19783	COX41_MOUSE	Cytochrome c oxidase subunit 4 isoform 1, mitochondrial	12	0.4
2.6	3	P68369	TBA1A_MOUSE	Tubulin alpha-1A chain	2	0.2
3.0	4	Q08857	CD36_MOUSE	Platelet glycoprotein 4	2	0.2

Table 2. Proteins from the skeletal muscle DRMs with altered expression *Dhcr7*$^{T93M/T93M}$ mice.

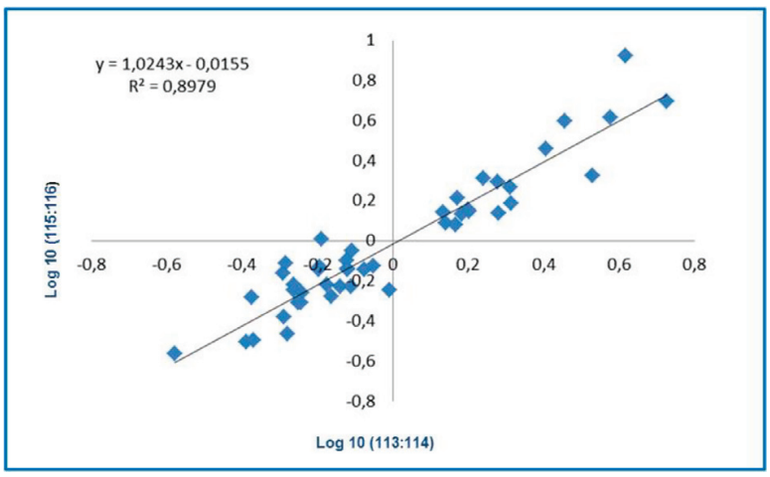

Figure 4. Comparison of the individual ratio values found for 38 proteins of DRMs extracted from skeletal muscle, which exhibited distinct levels of expression on hypomorphic *Dhcr7*$^{T93M/T93M}$ mice and wt-BL6 controls.

Proteins with altered expression corresponded to a number of biological processes. We found alterations affecting several membrane transporters. Even though no results from skeletal muscle studies of SLOS are available, membrane trafficking abnormalities, in other cells harboring inborn errors of cholesterol biosynthesis, had already been reported. For example, in cultivated human skin fibroblasts from SLOS patients the membrane fluidity is altered, calcium permeability is augmented whereas folate uptake and membrane-bound Na^+/K^+ ATPase activity are markedly decreased [33]. In agreement with these data, we now report decreased expression of phospholemman, a small plasma transmembrane protein that acts as a channel or channel regulator and modulates Na^+/K^+ ATPase activity [34, 35]. Further, we detected significantly decreased expression of another integral membrane glycoprotein associated with DRMs, the fatty acid translocase (FAT also called Cd36 or platelet glycoprotein 4) on

sarcolemma of SLOS mice, responsible for the uptake of long chain fatty acids [36–39]. Upregulated transporters include mitochondrial phosphate carrier protein (which transports inorganic phosphate into the mitochondrial matrix, essential for the aerobic synthesis of ATP) and ADP/ATP translocases 1 and 2 (that catalyzes the exchange of cytoplasmic ADP with mitochondrial ATP across the mitochondrial inner membrane).

These abnormalities of mitochondrial transporters may be indicative of more generalized defect in mitochondrial function and ATP production. Decreased expression of subunits corresponding to complexes I, III and IV of the oxidative phosphorylation (OXPHOS) system was observed, while four ATP-synthase subunits showed increased expression (ATP synthase mitochondrial subunits alpha, beta, delta and b1). Despite their mitochondrial origin, these proteins should not be considered as contaminants of DRMs preparations. Several biochemistry and proteomic studies had already shown the presence of complex I and ATP-synthase subunits in DRMs, [40, 41] and Poston showed that Triton X-114-resistant DRMs are also present in mitochondria and contain proteins that facilitate ATP production and export from this organelle [23], compatible with the increasing evidence of the presence of raft-like microdomains in mitochondria [21, 42].

Ca^{2+} is one of the most important signaling compounds involved in various cellular processes being intracellular Ca^{2+} levels tightly regulated by specialized proteins in the plasma membrane, sarcoplasmic reticulum (SR) and mitochondria [43]. Recent studies suggest that membrane rafts are involved in coordinating the protein interactions required for proper Ca^{2+} exchange between the MAM and mitochondria [23]. In the present study, we found increased expression of four membrane proteins related with Ca^{2+} homeostasis namely: annexin A2, sarcoplasmic/endoplasmic reticulum calcium ATPase 1 (SERCA1), calsequestrin-1 (CASQ1) and stromal interaction molecule 1 (STIM1).

Annexin A2 is a calcium-regulated membrane-binding protein, which holds two calcium ions. It has been proposed that it could play a key role in many processes including, (1) endocytosis and (2) exocytosis, (3) ion channel conductance, (4) link of F-actin cytoskeleton to the plasma membrane, (5) membrane organization, (6) formation of membrane cholesterol-rich microdomains and (7) regulation of cellular redox [44–46]. By LC-MS/MS, we found that annexin A2 was six times more abundant in DRMs obtained from *Dhcr7*$^{T93M/T93M}$ mice than in wt-BL6 and then confirmed such difference by immunocytochemistry (**Figure 5**).

It is possible that the presence of 7DHC in SLOS mice membranes drives a higher annexin A2 incorporation in microdomains since 7DHC may promote microdomain formation [47]. An alternate hypothesis would be that increased annexin A2 expression is related to its role in the regulation of redox potential. In fact, several data suggest an increase of oxidative stress in SLOS: (1) over a dozen of oxysterols have been produced from 7DHC by free radical oxidation in solution [48], (2) the oxysterol mixture derived from 7DHC free radical oxidation is biologically active and leads to morphological changes in Neuro2a cells treated with these oxysterols [49], (3) the synthesis of 3β,5α-dihydroxycholest-7-en-6-one (DHCEO), an oxysterol recently identified as a biomarker of 7DHC oxidation (in fibroblasts from SLOS patients and brain tissue), was found to be inhibited by an antioxidant compound in SLOS fibroblasts [47], (4) retinas from a SLOS rat model contain high levels of lipid hydroperoxides [50], (5) 7DHC

http://dx.doi.org/10.5772/intechopen.78037

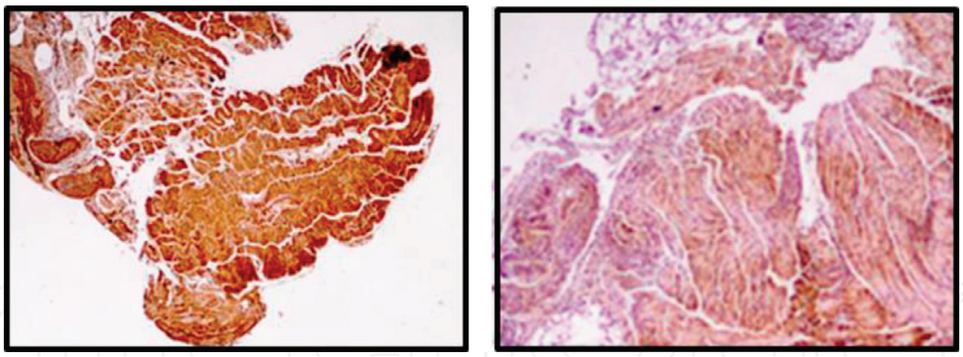

Figure 5. Immunohistochemical stain for annexin A2 (×4). Skeletal muscle samples of *Dhcr7*$^{93M/93M}$ (left) and wt-BL6 (right). The *Dhcr7*$^{93M/93M}$ (SLOS) sample shows a clear stronger coloration.

peroxidation is a major source of oxysterols observed in cells [51] and (6) we previously identified a significant increase of the antioxidant enzyme superoxide dismutase mitochondrial in cultivated human SLOS fibroblasts. Considering these facts, we can hypothesize that there is an alteration of redox state of the cells in SLOS and annexin 2 is overexpressed as a part of cell strategy to compensate such a situation and protect cells' biological compounds from peroxidation.

Another Ca^{2+} binding protein found upregulated in SLOS was SERCA1 an intracellular pump located in the SR of muscle cells, which catalyzes the hydrolysis of ATP coupled with the translocation of Ca^{2+} from the cytosol to the SR lumen, thus contributing to calcium sequestration involved in muscular excitation/contraction process. Another protein from this group is CASQ1, the major Ca^{2+}-binding protein in the skeletal muscle SR. CASQ1 acts as an internal calcium store in muscle. The release of calcium bound to this protein through a calcium release channel triggers muscle contraction. Finally, stromal interaction molecule is a transmembrane protein essential for the activation of store-operated Ca^{2+} entry (SOCE), a major Ca^{2+} influx mechanism.

We also found integrin beta-1, overexpressed in affected mice. This microdomain-associated protein belongs to the integrin family which incorporates heterodimeric transmembrane proteins that function as major receptors for extracellular matrix proteins [52]. Integrin beta-1, plays a role in the maintenance of the cytoarchitecture of mature muscle as well as in the functional integrity of the muscle cells and is present at the neuromuscular junctions in skeletal muscle ones [53]. One wonders if its overexpression could be one of the factors which protect skeletal muscle from severe dysfunction in SLOS in opposition to other organs.

Ordered domains are formed when actin filaments attach to the plasma membrane [54]. Kwik and collaborators found changes in the organization and activity of actin and actin-modifying proteins after cholesterol depletion, and Gangully and Chattopadhyay demonstrated that cholesterol depletion mimics the effect of cytoskeletal destabilization [55, 56]. Differences in myofilaments and cytoskeleton proteins were also suspected in our study.

Furthermore, some of the proteins identified were not so far, according to the available bibliography, associated with lipid-rafts or MAMs; nevertheless, they are involved in intracellular

physical connections like cytoskeleton-associated protein 4 (CKAP4) which is a transmembrane protein that further to its function as receptor also links endoplasmic reticulum (ER) to the cytoskeleton [57]. It is predictable that a membrane compact microdomain be involved in such function, in order to provide further support to the anchor. Such hypothesis is sustained by the fact that CKAP4 is a reversibly palmitoylated protein [58], and it is well described that palmitoylation of cytoplasmic proteins regulates the interaction of these soluble proteins with specific membranes or membrane domains. It is possible that palmitoylation controls the conformation of transmembrane segments, to modify the affinity of a membrane protein for specific membrane domains and to control protein–protein interactions [59].

Finally one should consider that both lipids and proteins for microdomains constructs are synthesized in the ER/Golgi before transport to the plasma membrane and, indeed, those proteins can be in a detergent-resistant, cholesterol-dependent state while residing there or in vesicle trafficking [60].

4. Conclusion

Our purpose was to contribute to the biological characterization of this *Dhcr7*$^{T93M/T93M}$ hypomorphic mouse model and identify differences that could help to go deeper in the understanding of SLOS physiopathology.

Proteomic analysis of DRMs of skeletal muscular samples clearly show differences between SLOS and wild-type mice, concerning proteins linked to membranes. The employed methodology allowed us to identify further alterations related with calcium homeostasis and membrane trafficking associated with SLOS and detected, for the first time, changes in mitochondrial energy metabolism in this mouse model.

To the best of our knowledge, this is the first research study focusing on the skeletal muscle of SLOS. The differential protein expression profile identified will open the way to comparative studies with more severally affected disease mice models as well as to similar approaches in human cells which may be helpful to uncover cellular mechanisms related to SLOS.

Acknowledgements

The authors are thankful to Prof Forbes D. Porter and Doctor Christopher A. Wassif from NIH who kindly provided the genetically modified mice model of SLOS used in this investigation. FDP and CAW are supported by the intramural research program of 30 the Eunice Kennedy Shriver National Institute of Child Health and Human Development.

Requimte received finnantial support from the European Union (FEDER funds POCI/01/0145/FEDER/007265) and National Funds (FCT/MEC, Fundação para a Ciência e Tecnologia and Ministério da Educação e Ciência) under the Partnership Agreement PT2020 UID/QUI/50006/2013.

This work received financial support from FCT/MEC through national funds and co-financed by FEDER, under the Partnership Agreement PT2020 (UID/MULTI/04378/2013 – POCI/01/0145/FERDER/007728).

Conflict of interest

The authors declare that there are no conflicts of interest.

Abbreviations

Cd36	cluster differentiation 36
BHT	butylhydroxytoluene; 2,6-bis(tert-butyl)-4-methylphenol
BSTFA	N,O-bis(trimethylsilyl)trifluoroacetamide
CASQ1	calsequestrin-1
α-CHCA	α-cyano-4-hydroxycinnamic acid
CHAPS	3-[(3-cholamidopropyl)dimethylammonio]-1-propanesulfonate
D	Day
7DHC	7-dehydrocholesterol
DHCEO	3β,5α-dihydroxycholest-7-en-6-one
7-DHCR	7-dehydrocholesterol redutase
EDTA	ethylenediaminetetraacetic acid
ER	endoplasmic reticulum
HEPES	4-(2-hydroxyethyl)-1-piperazineethanesulfonic acid
iTRAQ	isobaric tagging reagents
DRMs	detergent-resistant membranes
FAT	fatty acid translocase
GTP	guanine triphosphate
LCFAs	long-chain fatty acids
MMTS	S-methyl-methanethiosulfonate
mt-DNA	mitochondrial DNA

OXPHOS	oxidative phosphorylation
PBS	phosphate buffered saline
PIP2	phosphatidylinositol-4,5-biphosphate
SLOS	Smith-Lemli-Opitz syndrome
Dhcr7$^{T93M/T93M}$	Smith-Lemli-Opitz syndrome mouse, homozygous for T93M mutation
SR	sarcoplasmic reticulum
STIM1	stromal interaction molecule 1
TEAB	bicarbonate salt of triethylamine
TCEP	tris(2-carboxyethyl)phosphine hydrochloride
TFA	trifluoroacetic acid
UC	ultra-centrifuge
VDAC	voltage dependent anion-selective channels
wt-BL6	wild-type C57/BL6

Author details

Maria Luís Cardoso[1,2,3]*, Rui Vitorino[4], Henrique Reguengo[1,5], Susana Casal[6], Rui Fernandes[7], Isabel Duarte[7], Sofia Lamas[7], Renato Alves[4], Francisco Amado[4] and Franklim Marques[8]

*Address all correspondence to: m.luis.cardoso@insa.min-saude.pt

1 Faculty of Pharmacy, University of Porto, Porto, Portugal

2 National Health Institute Doutor Ricardo Jorge (INSA), Lisbon, Portugal

3 BioISI-Biosystems and Integrative Sciences Institute, University of Lisbon, Lisbon, Portugal

4 Department of Chemistry, QOPNA, Mass Spectrometry Center, University of Aveiro, Portugal

5 Department of Clinical Chemistry, Porto Hospital Center, Portugal

6 LAQV-REQUIMTE, Laboratory of Biochemistry, Department of Biological Sciences, Faculty of Pharmacy, University of Porto, Porto, Portugal

7 Institute for Molecular and Cell Biology, University of Porto, Porto, Portugal

8 UCIBIO-REQUIMTE, Laboratory of Biochemistry, Department of Biological Sciences, Faculty of Pharmacy, University of Porto, Porto, Portugal

References

[1] Porter FD, Herman GE. Malformation syndromes caused by disorders of cholesterol synthesis. Journal of Lipid Research. 2011;**52**(1):6-34

[2] Cardoso M, Barbosa M, Serra D, Martins E, Fortuna A, Reis-Lima M, Bandeira A, Balreira A, Marques F. Living with inborn errors of cholesterol biosynthesis: Lessons from adult patients. Clinical Genetics. 2014;**85**(2):184-188

[3] Smith DW, Lemli L, Opitz JA. A newly recognized syndrome of multiple congenital anomlies. The Journal of Pediatrics. 1964;**64**:210-217

[4] Irons M, Elias ER, Salen G, Tint GS, Batta AK. Defective cholesterol biosynthesis in Smith-Lemli-Opitz syndrome. Lancet. 1993;**341**(8857):1414

[5] Tint GS. Cholesterol defect in Smith-Lemli-Opitz syndrome. American Journal of Medical Genetics. 1993;**47**(4):573-574

[6] Fitzky BU, Witsch-Baumgartner M, Erdel M, Lee JN, Paik YK, Glossmann H, Utermann G, Moebius FF. Mutations in the Delta7-sterol reductase gene in patients with the Smith-Lemli-Opitz syndrome. Proceedings of the National Academy of Sciences of the United States of America. 1998;**95**(14):8181-8186

[7] Wassif CA, Maslen C, Kachilele-Linjewile S, Lin D, Linck LM, Connor WE, Steiner RD, Porter FD. Mutations in the human sterol delta7-reductase gene at 11q12-13 cause Smith-Lemli-Opitz syndrome. American Journal of Human Genetics. 1998;**63**(1):55-62

[8] Waterham HR, Wijburg FA, Hennekam RC, Vreken P, Poll-The BT, Dorland L, Duran M, Jira PE, Smeitink JA, Wevers RA, Wanders RJ. Smith-Lemli-Opitz syndrome is caused by mutations in the 7-dehydrocholesterol reductase gene. American Journal of Human Genetics. 1998;**63**(2):329-338

[9] Waterham HR, Hennekam RC. Mutational spectrum of Smith-Lemli-Opitz syndrome. American Journal of Medical Genetics. Part C, Seminars in Medical Genetics. 2012;**160C**(4):263-284

[10] Fitzky BU, Moebius FF, Asaoka H, Waage-Baudet H, Xu L, Xu G, Maeda N, Kluckman K, Hiller S, Yu H, Batta AK, Shefer S, Chen T, Salen G, Sulik K, Simoni RD, Ness GC, Glossmann H, Patel SB, Tint GS. 7-Dehydrocholesterol-dependent proteolysis of HMG-CoA reductase suppresses sterol biosynthesis in amouse model of Smith-Lemli-Opitz/RSH syndrome. The Journal of Clinical Investigation. 2001;**108**(6):905-915

[11] Wassif CA, Zhu P, Kratz L, Krakowiak PA, Battaile KP, Weight FF, Grinberg A, Steiner RD, Nwokoro NA, Kelley RI, Stewart RR, Porter FD. Biochemical, phenotypic and neuro-physiological characterization of a genetic mouse model of RSH/Smith-Lemli-Opitz syndrome. Human Molecular Genetics. 2001;**10**(6):555-564

[12] Correa-Cerro LS, Wassif CA, Kratz L, Miller GF, Munasinghe JP, Grinberg A, Fliesler SJ, Porter FD. Development and characterization of a hypomorphic Smith-Lemli-Opitz syndrome mouse model and efficacy of simvastatin therapy. Human Molecular Genetics. 2006;**15**(6):839-851

[13] De Brasi D, Esposito T, Rossi M, Parenti G, Sperandeo MP, Zuppaldi A, Bardaro T, Ambruzzi MA, Zelante L, Ciccodicola A, Sebastio G, D'Urso M, Andria G. Smith-Lemli-Opitz syndrome: Evidence of T93M as a common mutation of delta7-sterol reductase in Italy and report of three novel mutations. European Journal of Human Genetics. 1999;**7**(8):937-940

[14] Nowaczyk MJ, Martin-Garcia D, Aquino-Perna A, Rodriguez-Vazquez M, McCaughey D, Eng B, Nakamura LM, Waye JS. Founder effect for the T93M DHCR7 mutation in Smith-Lemli-Opitz syndrome. American Journal of Medical Genetics. Part A. 2004;**125A**(2):173-176

[15] Cardoso ML, Balreira A, Martins E, Nunes L, Cabral A, Marques M, Lima MR, Marques JS, Medeira A, Cordeiro I, Pedro S, Mota MC, Dionisi-Vici C, Santorelli FM, Jakobs C, Clayton PT, Vilarinho L. Molecular studies in Portuguese patients with Smith-Lemli-Opitz syndrome and report of three new mutations in DHCR7. Molecular Genetics and Metabolism. 2005;**85**(3):228-235

[16] Marcos J, Shackleton CH, Buddhikot MM, Porter FD, Watson GL. Cholesterol biosynthesis from birth to adulthood in a mouse model for 7-dehydrosterol reductase deficiency (Smith-Lemli-Opitz syndrome). Steroids. 2007;**72**(11–12):802-808

[17] Marin R, Fabelo N, Martín V, Garcia-Esparcia P, Ferrer I, Quinto-Alemany D, Díaz M. Anomalies occurring in lipid profiles and protein distribution in frontal cortex lipid rafts in dementia with Lewy bodies disclose neurochemical traits partially shared by Alzheimer's and Parkinson's diseases. Neurobiology of Aging. 2017;**49**:52-59

[18] Chichili GR, Rodgers W. Cytoskeleton-membrane interactions in membrane raft structure. Cellular and Molecular Life Sciences. 2009;**66**(14):2319-2328

[19] Zheng YZ, Foster LJ. Contributions of quantitative proteomics to understanding membrane microdomains. Journal of Lipid Research. 2009;**50**(10):1976-1985

[20] Hayashi T, Fujimoto M. Detergent-resistant microdomains determine the localization of sigma-1 receptors to the endoplasmic reticulum-mitochondria junction. Molecular Pharmacology. 2010;**77**(4):517-528

[21] Ciarlo L, Manganelli V, Garofalo T, Matarrese P, Tinari A, Misasi R, Malorni W, Sorice M. Association of fission proteins with mitochondrial raft-like domains. Cell Death and Differentiation. 2010;**17**(6):1047-1058

[22] Garofalo T, Manganelli V, Grasso M, Mattei V, Ferri A, Misasi R, Sorice M. Role of mitochondrial raft-like microdomains in the regulation of cell apoptosis. Apoptosis. 2015; (5):621-634

[23] Poston CN, Duong E, Cao Y, Bazemore-Walker CR. Proteomic analysis of lipid raft-enriched membranes isolated from internal organelles. Biochemical and Biophysical Research Communications. 2011;**415**(2):355-360

[24] Fuller HR, Man NT, Lam le T, Shamanin VA, Androphy EJ, Morris GE. Valproate and bone loss: iTRAQ proteomics show that valproate reduces collagens and osteonectin in SMA cells. Journal of Proteome Research. 2010;**9**(8):4228-4233

[25] Shi M, Hwang H, Zhang J. Quantitative characterization of glycoproteins in neurodegenerative disorders using iTRAQ. Methods in Molecular Biology. 2013;**951**:279-296

[26] Kroksveen AC, Aasebø E, Vethe H, Van Pesch V, Franciotta D, Teunissen CE, Ulvik RJ, Vedeler C, Myhr KM, Barsnes H, Berven FS. Discovery and initial verification of differentially abundant proteins between multiple sclerosis patients and controls using iTRAQ and SID-SRM. Journal of Proteomics. 2013;**78**:312-325

[27] Hou G, Wang Y, Lou X, Liu S. Combination strategy of quantitative proteomics uncovers the related proteins of colorectal cancer in the interstitial fluid of colonic tissue from the AOM-DSS mouse model. Methods in Molecular Biology. Nov 15, 2017. pp. 1-8. DOI: 10.1007/7651_2017_88

[28] Kim KB, Lee JS, Ko YG. The isolation of detergent-resistant lipid rafts for two-dimensional electrophoresis. Methods in Molecular Biology. 2008;**424**:413-422

[29] Amaral C, Gallardo E, Rodrigues R, Pinto Leite R, Quelhas D, Tomaz CL. Quantitative analysis of five sterols in amniotic fluid by GC-MS: Application to the diagnosis of cholesterol biosynthesis defects. Journal of Chromatography. B, Analytical Technologies in the Biomedical and Life Sciences. 2010;**878**(23):213

[30] Vitorino R, Barros A, Caseiro A, Domingues P, Duarte J, Amado F. Towards defining the whole salivary peptidome. Proteomics Clinical Applications. 2009;**3**(5):528-540

[31] Vitorino R, Guedes S, Manadas B, Ferreira R, Amado F. Toward a standardized saliva proteome analysis methodology. Journal of Proteomics. 2012;**75**(17):5140-5165

[32] Rakheja D, Boriack RL. Precholesterol sterols accumulate in lipid rafts of patients with Smith-Lemli-Opitz syndrome and X-linked dominant chondrodysplasia punctata. Pediatric and Developmental Pathology. 2008;**11**(2):128-132

[33] Tulenko TN, Boeze-Battaglia K, Mason RP, Tint GS, Steiner RD, Connor WE, Labelle EF. A membrane defect in the pathogenesis of the Smith-Lemli-Opitz syndrome. Journal of Lipid Research. 2006;**47**(1):134-143

[34] Bogaev RC, Jia LG, Kobayashi YM, Palmer CJ, Mounsey JP, Moorman JR, Jones LR, Tucker AL. Gene structure and expression of phospholemman in mouse. Gene. 2001; **271**(1):69-79

[35] Banine F, Matagne V, Sherman LS, Ojeda SR. Brain region-specific expression of Fxyd1, an Mecp2 target gene, is regulated by epigenetic mechanisms. Journal of Neuroscience Research. 2011;**89**(6):840-851. DOI: 10.1002/jnr.22608

[36] Zeng Y, Tao N, Chung KN, Heuser JE, Lublin DM. Endocytosis of oxidized low density lipoprotein through scavenger receptor CD36 utilizes a lipid raft pathway that does not require caveolin-1. The Journal of Biological Chemistry. 2005;**278**(46):45931-45936

[37] Pohl J, Ring A, Korkmaz U, Ehehalt R, Stremmel W. FAT/CD36-mediated long-chain fatty acid uptake in adipocytes requires plasma membrane rafts. Molecular Biology of the Cell. 2005;**16**(1):24-31

[38] Harasim E, Kalinowska A, Chabowski A, Stepek T. The role of fatty-acid transport proteins (FAT/CD36, FABPpm, FATP) in lipid metabolism in skeletal muscles. Post® py Higieny i Medycyny Doświadczalnej (Online). 2008;**25**(62):433-441

[39] Schwenk RW, Holloway GP, Luiken JJ, Bonen A, Glatz JF. Fatty acid transport across the cell membrane: Regulation by fatty acid transporters. Prostaglandins, Leukotrienes, and Essential Fatty Acids. 2010;**82**(4–6):149-154

[40] Kim BW, Lee JW, Choo HJ, Lee CS, Jung SY, Yi JS, Ham YM, Lee JH, Hong J, Kang MJ, Chi SG, Hyung SW, Lee SW, Kim HM, Cho BR, Min DS, Yoon G, Ko YG. Mitochondrial oxidative phosphorylation system is recruited to detergent-resistant lipid rafts during myogenesis. Proteomics. 2010;**10**(13):2498-2515

[41] Devenish RJ, Prescott M, Rodgers AJ. The structure and function of mitochondrial F1F0-ATP synthases. International Review of Cell and Molecular Biology. 2008;**267**:1-58

[42] Sorice M, Mattei V, Tasciotti V, Manganelli V, Garofalo T, Misasi R. Trafficking of PrPc to mitochondrial raft-like microdomains during cell apoptosis. Prion. 2012;**6**(4):354-358

[43] Krapivinsky G, Krapivinsky L, Stotz SC, Manasian Y, Clapham DE. POST, partner of stromal interaction molecule 1 (STIM1), targets STIM1 to multiple transporters. Proceedings of the National Academy of Sciences of the United States of America. 2011;**108**(48): 19234-19239

[44] Bharadwaj A, Bydoun M, Holloway R, Waisman D. Annexin A2 heterotetramer: Structure and function. International Journal of Molecular Sciences. 2013;**14**(3):6259-6305

[45] Madureira PA, Waisman DM. Annexin A2: The importance of being redox sensitive. International Journal of Molecular Sciences. 2013;**14**(2):3568-3594

[46] Chasserot-Golaz S, Vitale N, Umbrecht-Jenck E, Knight D, Gerke V, Bader MF. Annexin 2 promotes the formation of lipid microdomains required for calcium-regulated exocytosis of dense-core vesicles. Molecular Biology of the Cell. 2005;**16**(3):1108-1119

[47] Xu X, Bittman R, Duportail G, Heissler D, Vilcheze C, London E. Effect of the structure of natural sterols and sphingolipids on the formation of ordered sphingolipid/sterol domains (rafts). Comparison of cholesterol to plant, fungal, and disease-associated sterols and comparison of sphingomyelin, cerebrosides, and ceramide. Journal of Biological Chemistry. 2001;**276**(36):33540-33546

[48] Xu L, Korade Z, Rosado DA Jr, Liu W, Lamberson CR, Porter NA. An oxysterol biomarker for 7-dehydrocholesterol oxidation in cell/mouse models for Smith-Lemli-Opitzsyndrome. Journal of Lipid Research. 2011;**52**(6):1222-1233

[49] Korade Z, Xu L, Shelton R, Porter NA. Biological activities of 7-dehydrocholesterol-derived oxysterols: Implications for Smith-Lemli-Opitz syndrome. Journal of Lipid Research. 2010;**51**:3259-3269

[50] Richards MJ, Nagel BA, Fliesler SJ. Lipid hydroperoxide formation in the retina: Correlation with retinal degeneration and light damage in a rat model of smith-Lemli-Opitz syndrome. Experimental Eye Research. 2006;**82**(3):538-541

[51] Xu L, Korade Z, Rosado DA Jr, Mirnics K, Porter NA. Metabolism of oxysterols derived from nonenzymatic oxidation of 7-dehydrocholesterol in cells. Journal of Lipid Research. 2013;**54**(4):1135-1143

[52] Wang C, Yoo Y, Fan H, Kim E, Guan KL, Guan JL. Regulation of integrin β 1 recycling to lipid rafts by Rab1a to promote cell migration. The Journal of Biological Chemistry. 2010; **285**(38):29398-29405

[53] van der Flier A, Gaspar AC, Thorsteinsdóttir S, Baudoin C, Groeneveld E, Mummery CL, Sonnenberg A. Spatial and temporal expression of the beta1D integrin during mouse development. Developmental Dynamics. 1997;**210**(4):472-486

[54] Dinic J, Ashrafzadeh P, Parmryd I. Actin filaments attachment at the plasma membrane in live cells cause the formation of ordered lipid domains. Biochimica et Biophysica Acta. 2013;**1828**(3):1102-1111

[55] Kwik J, Boyle S, Fooksman D, Margolis L, Sheetz MP, Edidin M. Membrane cholesterol, lateral mobility, and the phosphatidylinositol 4,5-bisphosphate-dependent organization of cell actin. Proceedings of the National Academy of Sciences. 2003;**100**(24):13964-13969

[56] Ganguly S, Chattopadhyay A. Cholesterol depletion mimics the effect of cytoskeletal destabilization on membrane dynamics of the serotonin1A receptor: A zFCS study. Biophysical Journal. 2010;**99**(5):1397-1407

[57] Planey SL, Keay SK, Zhang CO, Zacharias DA. Palmitoylation of cytoskeleton associated protein 4 by DHHC2 regulates antiproliferative factor-mediated signaling. Molecular Biology of the Cell. 2009;**20**(5):1454-1463

[58] Zacharias DA, Mullen M, Planey SL. Antiproliferative factor-induced changes in phosphorylation and palmitoylation of cytoskeleton-associatedprotein-4 regulate its nuclear translocation and DNA binding. International Journal of Cell Biology. 2012;**2012**:150918

[59] Charollais J, Van Der Goot FG. Palmitoylation of membrane proteins (review). Molecular Membrane Biology. 2009;**26**(1):55-66

[60] Dave RH, Saengsawang W, Yu J-Z, Donati R, Rasenick MM. Heterotrimeric G-proteins interact directly with cytoskeletal components to modify microtubule-dependent cellular processes. Neuro-Signals. 2009;**17**(1):100-108

IntechOpen